ARTICLE
Journal of Cellular Biochemistry 113:1122–1131 (2012)

Journal of Cellular Biochemistry

PI3K/Akt-Dependent Functions of TFII-I Transcription Factors in Mouse Embryonic Stem Cells

Nyam-Osor Chimge,[1] Aleksandr V. Makeyev,[1] Sabine J. Waigel,[2] Badam Enkhmandakh,[1] and Dashzeveg Bayarsaihan[1*]

[1]*Department of Reconstructive Sciences, Center for Regenerative Medicine and Skeletal Development, School of Dentistry, University of Connecticut Health Center, 262 Farmington Avenue, Farmington, CT 06030*

[2]*Brown Cancer Center, University of Louisville, Louisville, KY 40202*

ABSTRACT

Activation of PI3K/Akt signaling is sufficient to maintain the pluripotency of mouse embryonic stem cells (mESC) and results in down-regulation of *Gtf2i* and *Gtf2ird1* encoding TFII-I family transcription factors. To investigate how these genes might be involved in the process of embryonic stem cell differentiation, we performed expression microarray profiling of mESC upon inhibition of PI3K by LY294002. This analysis revealed significant alterations in expression of genes for specific subsets of chromatin-modifying enzymes. Surprisingly, genome-wide promoter ChIP-chip mapping indicated that the majority of differently expressed genes could be direct targets of TFII-I regulation. The data support the hypothesis that upregulation of TFII-I factors leads to activation of a specific group of developmental genes during mESC differentiation. J. Cell. Biochem. 113: 1122–1131, 2012.

KEY WORDS: EMBRYONIC STEM CELLS; *Gtf2i*; *Gtf2ird1*; EPIGENETICS; TFII-I; PHOSPHOINOSITOL 3-KINASE

TFII-I and BEN belong to a family of multifunctional transcription factors involved in regulation of a number of genes during embryonic development [Chimge et al., 2008; Enkhmandakh et al., 2009]. Haploinsufficiency for *GTF2I* and *GTF2IRD1*, which encode these proteins, is believed to be the primary cause for facial dysmorphism and cognitive defects in Williams–Beuren syndrome patients [Tassabehji et al., 2005; Enkhmandakh et al., 2009; Ferrero et al., 2010].

Immunohistochemical analysis revealed broad and extensive expression of TFII-I and BEN during very early mouse pre- and postimplantation development [Bayarsaihan et al., 2003; Enkhmandakh et al., 2004]. The maternally expressed proteins were first detected in the cytoplasm and pronuclei of the zygote. At the two-cell stage, when zygotic gene activation begins, TFII-I and BEN preferentially localize in the nucleus. This expression pattern remained basically unchanged throughout the stages of cleavage and compaction (8-, 16-cell, morula, and early blastocyst stages). However, at the stage of implantation (E4.5), BEN is mostly detected in the cytoplasm of trophoblast cells [Bayarsaihan et al., 2003], but TFII-I is localized in the cytoplasm and nuclei of the inner cell mass (ICM), as well as in trophectoderm [Enkhmandakh et al., 2004]. Consistently, whole mount in situ hybridization of blastocysts prior to implantation showed highly enriched ICM-predominant localization of TFII-I mRNA [Yoshikawa et al., 2006]. Although TFII-I transcription factors are expressed in mouse embryonic stem cells (mESC), they are not necessary for maintenance of pluripotency because both *Gtf2i* and *Gtf2ird1* deficient mouse embryos survive the gastrulation stage [Enkhmandakh et al., 2009].

Phosphatidylinositol 3-kinase (PI3K)/Akt is one of the major signaling pathways involved in both mouse and human ESC maintenance [Stewart et al., 2008]. LY294002 is cell-permeable, potent, and specific PI3K inhibitor that acts on the ATP-binding site of the enzyme [Djordjevic and Driscoll, 2002]. LY294002-induced mESC differentiation was chosen based on the following observations: (i) use of either 5 μM LY294002 or expression of a dominant-negative class IA PI3K mutant in the presence of leukemia inhibitory factor (LIF) led to the loss of self-renewal of mESC [Paling et al., 2004], (ii) myristoylated, active form of Akt is sufficient to maintain pluripotency in mouse and human ESC without the addition of LIF [Watanabe et al., 2006], and (iii) activation of Akt signaling in mESC in the absence or presence of LIF significantly (more than twofold) down-regulates expression of *Gtf2i* gene (GEO record GDS1616).

Additional Supporting Information may be found in the online version of this article.

Grant sponsor: National Institute of Dental and Craniofacial Research, NIDCR; Grant numbers: R01DE017205, K02DE18412; Grant sponsor: Connecticut Stem Cell Grant; Grant number: 09-SCB-UCHC.

*Correspondence to: Dashzeveg Bayarsaihan, Department of Reconstructive Sciences, Center for Regenerative Medicine and Skeletal Development, School of Dentistry, University of Connecticut Health Center, 262 Farmington Avenue, Farmington, CT 06030. E-mail: dashzeveg@uchc.edu

Received 4 September 2011; Accepted 1 November 2011 • DOI 10.1002/jcb.23441 • © 2011 Wiley Periodicals, Inc.
Published online 17 November 2011 in Wiley Online Library (wileyonlinelibrary.com).

In our effort to elucidate the role of TFII-I and BEN in differentiation, we performed genome-wide expression profiling of mESC upon inhibition of PI3K by LY294002 combined with siRNA knockdown of TFII-I proteins. Statistical analysis of the resulting data has defined a set of genes, expression of which could be dependent on TFII-I and BEN in differentiating mESC.

MATERIALS AND METHODS

CELL CULTURE MAINTENANCE AND DIFFERENTIATION

Mouse E14tg2a embryonic stem cells were obtained from the ATCC (CRL-1821). mESC were grown in a feeder-free environment in KDMEM (Invitrogen, Carlsbad, CA) containing 15% knockout serum replacement (Gibco), 1000 U/ml *LIF* (Chemicon, Temecula, CA), 0.1 μM non-essential amino acids, penicillin-streptomycin-L-glutamine and 2-mercaptoethanol. For inhibition of PI3K pathway E14tg2a cells were plated at 10^5 cell density in six well plates and treated with 5 μM LY294002 (Enzo Life Sciences, Farmingdale, NY) in the presence of LIF. Control samples were treated with solvent only. Cell-associated alkaline phosphatase activity was determined using a commercially available kit (ALP-10, Sigma-Aldrich, St. Louis, MO). Briefly, test cell populations were washed twice in PBS, lysed in 0.1% Triton X for 5 min prior to addition of the *p*-nitrophenyl phosphate buffer.

siRNA KNOCKDOWN OF TFII-I PROTEINS

For knockdown purposes cells were transfected with ON-TARGETplus SMARTpool siRNA for *Gtf2i* and *Gtf2ird1*, and ON-TARGET*plus* Non-targeting Pool (Dharmacon, Lafayette, CO), respectively. Three independent transfections have been performed in the presence of LIF and LY294002 for each gene as well as for negative control siRNA using *DharmaFECT 1* (Dharmacon) transfection reagent. Twenty-four hours after siRNA knockdown cells from all experimental and control samples were collected for RNA isolation.

RNA ISOLATION AND QUANTITATION

Total RNA was isolated with RNeasy kit (Qiagen, Germantown, MD) according to the manufacturer's instructions. RNA concentration was determined using a NanoDrop® ND-1000 spectrophotometer (NanoDrop Technologies, Wilmington, DE). The RNA Integrity Number (RIN) determined by the Agilent Bioanalyzer 2100 (Agilent Technologies, Inc., Santa Clara, CA) was used as a measure of the RNA quality.

ChIP-Chip

ES E14tg2a cells and Ainv15 cells expressing Tet-inducible HA-tagged BEN were crosslinked and chromatin was prepared from those cells using the ChIP-IT kit (Active Motif, Carlsbad, CA) according to the manufacturer's protocol. ChIP experiment was performed with goat anti-BEN polyclonal IgG M-19, goat anti-TFII-I polyclonal IgG V-18, mouse anti-HA monoclonal IgG2b 12CA5 (sc-14714X, sc-9943X, and sc-57592, Santa Cruz Biotechnology, Santa Cruz, CA, respectively) and with rabbit anti-TFII-I polyclonal antibodies (4562, Cell Signaling, Danvers, MA) and antibody–chromatin complexes were purified using protein G-coated magnetic beads (Active Motif). After reverse cross-links and purification on QIAquick spin columns (Qiagen), immunoaffinity-enriched DNA fragments (IP) and the input samples were amplified using whole-genome GenomePlex Complete WGA kit (Sigma–Aldrich, MO). IP and input samples were labeled in separate reactions with Cy5 and Cy3, respectively, and then were co-hybridized to Mouse 385K RefSeq Promoter Arrays (Roche NimbleGen, Madison, WI). Data were extracted using NimbleScan software and peaks were detected by searching for four or more probes with a signal above a cut-off value using a 500-bp sliding window. Log_2 ratios of IP versus input sample were calculated, and mapping to the transcription start sites of genes was performed using SignalMap software (Roche NimbleGen).

MICROARRAY AND DATA ANALYSIS

The labeling of RNA samples was performed using Affymetrix GeneChip 3′IVT express kit (Affymetrix Inc., Santa Clara, CA) as described in the users guide kit. A total of 50 ng of RNA per each replicate was used for labeling. The reaction utilizes linear RNA amplification to yield biotinylated targets from the 3′ end and uses ArrayScript™ reverse transcription to synthesize cDNA. RNA is generated using MEGAscript in vitro transcription technology and is purified using magnetic beads for higher recovery yields. The target cRNAs were fragmented, combined with hybridization, and spike controls and hybridized to the high-density Mouse Genome 430 2.0 GeneChip (Affymetrix, Inc.) that offers comprehensive analysis of genome-wide expression on a single array. The labeling, hybridization, scanning, and raw data analysis were done at the Microarray Facility of University of Louisville.

For the raw data analysis Affymetrix CEL files were imported into Partek Genomics Suite™ 6.4 (Partek Inc., St. Louis, MO) using the default normalization parameters. Probe-level data was processed using robust multi-array average (RMA) of background-adjusted, normalized, and log-transformed perfect match (PM) values. Differential expression analysis was performed using Partek software by two-way ANOVA analysis. The cutoff value for discrimination of false positives was at the significance level $P < 0.05$ and $P < 0.25$ corrected for the numbers of tests performed (corrected *P*-value).

Putative TFII-I and BEN binding sites were searched as a pattern consensus on both strands by using MacVector 9.5 (Oxford Molecular Group, Oxford, UK). Statistical analysis was performed by using InStat 3.0b (GraphPad Software Inc., La Jolla, CA).

QRT-PCR ANALYSIS

cDNA was synthesized from 2 μg of total RNA with Omniscript Reverse transcription kit (Qiagen) using oligo dT primers. Quantitative PCR was carried out on the ABI PRISM 7300 detection system (Applied Biosystems, Carlsbad, CA) in triplicate using commercially available pre-developed TaqMan gene expression assays (Applied Biosystems). Amplification specificity was assessed using both melt curve analysis and gel electrophoresis. All transcript levels were normalized to that of *Gapdh* and the relative expression ratios were calculated by using the $2^{-\Delta\Delta C_t}$ method of data analysis. Significance of change for individual genes was performed by using InStat 3.0b GraphPad Software (GraphPad Software).

RESULTS

INHIBITION OF PI3K/Akt SIGNALING RESULTED IN THE INCREASED EXPRESSION OF *Gtf2i* AND *Gtf2ird1*

We have previously noticed that activation of PI3K/Akt signaling in mESC in the absence or presence of LIF results in a significant down-regulation (more than twofold) of *Gtf2i* expression (GEO record GDS1616). To confirm that TFII-I genes are downstream of the PI3K/Akt signaling pathway we decided to look at the effect of inhibition of PI3K on TFII-I gene expression using LY294002, a well characterized specific PI3K inhibitor.

To select conditions for the LY294002 treatment, we compared time (9, 24, and 48 h) effects of this inhibitor on the *Gtf2i* and *Gtf2ird1* expression in mESC. It was previously reported that addition of LY294002 to the culture medium at a concentration of 5 μM leads to a loss of mESC self-renewal [Paling et al., 2004]. We noticed that the same treatment resulted in an increase of *Gtf2i* (2.8-fold) and *Gtf2ird1* (2.3-fold) expression at 9 h but weakens overtime. After 48 h of treatment expression levels of *Gtf2i* and *Gtf2ird1* were 1.6- and 1.5-fold, respectively as compared to solvent-only treated control cells (Fig. 1A). Treatment with LY294002 equally up-regulated α, β, Δ, and γ splice variants of *Gtf2i* (data not shown). Moreover our results were consistent with the microarray data [Watanabe et al., 2006] where Akt activation down-regulated expression of *Gtf2i* (GEO record GDS1616).

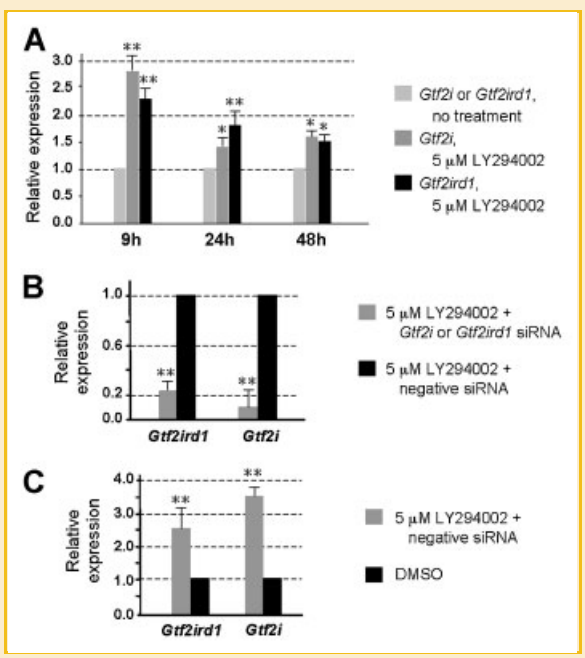

Fig. 1. qRT-PCR measurements of Gtf2i/TFII-I and Gtf2ird1/BEN expression in mESCs. A: Time-course of 5 μM LY294002 treatment. B: Effects of gene-specific siRNA silencing and (C) of 5 μM LY294002 treatment in RNA samples used for Affymetrix expression analysis after 9 h of LY294002 treatment. Error bars represent standard deviation calculated from three independent experiments. One and two asterisks indicate statistically significant fold of changes ($P < 0.05$ and $P < 0.01$, respectively).

The siRNA knockdown of *Gtf2i* and *Gtf2ird1* was performed in mESC after 9 h treatment with 5 μM LY294002, the time of their highest expression. qRT-PCR revealed the 6.6- and 3.1-fold decrease of *Gtf2i* and *Gtf2ird1* expression, respectively, as a result of siRNA knockdown (Fig. 1B). In contrast, comparison of the samples transfected with negative control siRNA with solvent-only treated samples revealed that LY294002 treatment induced 3.4- and 2.8-fold increases of *Gtf2i* and *Gtf2ird1* expression, respectively (Fig. 1C). We considered the combined LY294002/negative siRNA-treated samples to be equivalent to LY294002 treated ones assuming that negative siRNA transfection does not cause any significant changes.

Post-transcriptional silencing (knockdown) of TFII-I and BEN by gene-specific siRNAs did not induce any apparent abnormal morphology changes in mouse ESC after 24 h of treatment. Moreover, even double TFII-I/BEN knockdown has no effect on alkaline phosphatase staining, which is one of the criteria for ESC pluripotency (data not shown).

GENOME-WIDE CHANGES INDUCED BY LY294002 TREATMENT

To assess the global gene expression, we used Mouse Genome 430 2.0 Array containing more than 45,000 probe sets for over 39,000 transcripts and splice variants from over 34,000 well-characterized mouse genes.

Principal component analysis demonstrated that the LY294002 treatment caused substantial alteration in the expression profiling of mESC relative to the pluripotent control cells treated with DMSO solvent only while knockdown of TFII-I and BEN did not cause significant changes as compared to negative control siRNA knockdown (Fig. 2A). The inhibition of the PI3K/Akt signaling affected expression of 3,709 genes (*corr.* $P < 0.05$) as compared to the pluripotent control samples. Among them 1,772 genes were down-regulated and 1,937 were up-regulated. The list of altered genes with the highest fold changes is shown in Table I.

In agreement with the role of PI3K/Akt on cell proliferation and self-renewal, our study revealed differential expression of numerous genes involved in cell cycle regulation. Among catalytic subunits of the protein kinase complexes that are required for cell cycle G_1 phase progression, LY294002 treatment significantly decreased transcription of *Cdk6* but not *Cdk2* and *Cdk4*. Selective down-regulation was also observed of some regulatory subunits of D-type cyclins: LY29002 treatment resulted in inhibition of transcription of *Cyclin D1* and, to a much greater extent, *Cyclin D2* but did not affect expression of *Cyclin D3*, which is necessary for cell cycle progression through G2 phase into mitosis after UV radiation. LY294002 exerted little influence on expression of the Ink4 family of cyclin-dependent kinase inhibitors and prevented the activation of *Cdk4* and *Cdk6* but strongly repressed transcription of *Cyclin-dependent kinase inhibitors 1a* (*p21Cip1*) and *1c* (*Cdkn1c*) controlling the activity of cyclin-Cdk4/6 complexes (Supplemental Table I). LY294002 had no effect on expressions of *Cyclin E1* and *p27Kip1*, cyclin-dependent kinase inhibitor 1b, which prevents the activation of cyclin E-Cdk2 complexes.

Additionally, we observed changes in expression of genes of the LIF/JAK/STAT, TGFβ/BMP, and Wnt/β-catenin signaling pathways implicated in the maintenance of mESC. Remarkably, among genes

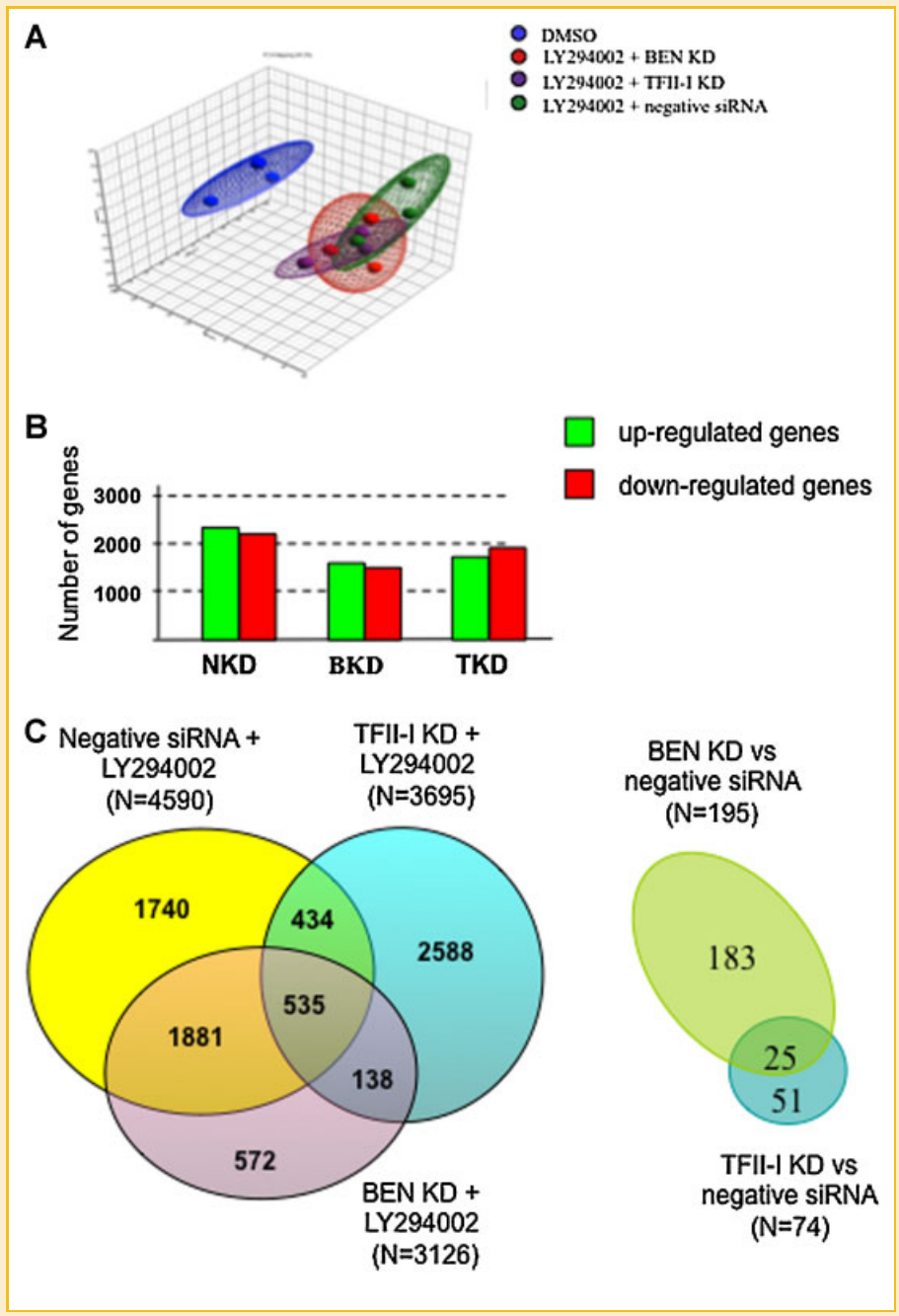

Fig. 2. Genome-wide changes induced in mESCs by LY294002 treatment and by abrogation of TFII-I proteins. A: Schematic representation of principal component analysis. B: Number of genes affected by treatment with 5 μM LY294002 in the presence of negative control siRNA (NKD), BEN knockdown (BKD), or TFII-I knockdown (TKD). (C) Venn diagrams of overlapping and differentially expressed genes in BEN and TFII-I knockdown experiments.

of the TGFβ pathway our results showed down-regulation of genes critical in the left-right asymmetry determination (*Thbs1*, *Lefty1*, *Lefty2*, and *Pitx2*).

LY29002 TREATMENT CHANGES EXPRESSION OF KEY CHROMATIN-MODIFYING ENZYME GENES

Analysis of the genome-wide changes induced by LY294002 also revealed significant alterations in expression of genes for specific subsets of chromatin-modifying enzymes. We have detected increased expression of *Suv39h1* that trimethylates histone H3 on Lys-9 (H3K9me3), whereas expression of another heterochromatin methyltransferase gene *Suv420h1*, which trimethylates histone H4 on Lys-20 (H4K20me3) was not changed. We also detected up-regulation of *Euchromatic histone lysine N-methyltransferase 2* (*Ehmt2*) and *Enhancer of zeste homolog 2* (*Ezh2*), but not *Ezh1*, a component of the Polycomb Repressive Complex 2 that mediates methylation of H3K27 and functions in the maintenance of ESC pluripotency and plasticity [Shen et al., 2008]. We noticed that

TABLE I. List of Up- and Down-Regulated Genes With the Highest Fold Change After Inhibiting PI3K/Akt Signaling

		Accession #	Fold change	*P*-value
Top up-regulated genes				
Empty spiracles homolog 2 (Drosophila)	*Emx2*	NM_010132	3.9	3.19E−07
Mannosidase 2, alpha B2	*Man2b2*	NM_008550	2.7	3.28E−03
Epithelial membrane protein 1	*Emp1*	NM_010128	2.6	7.48E−05
Solute carrier family 11	*Slc11a1*	NM_013612	2.5	3.07E−05
Trans-golgi network protein	*Tgoln1*	NM_009443	2.5	2.67E−04
TEA domain family member 4	*Tead4*	NM_011567	2.5	1.89E−04
CDC2-related kinase 7	*Crk7*	NM_026952	2.4	2.20E−05
Regulator of G-protein signaling 19 interacting protein 1	*Rgs19ip1*	NM_018771	2.3	5.31E−06
Plexin domain containing 1	*Plxdc1*	NM_028199	2.3	2.69E−05
Zinc finger, matrin type 4	*Zmat4*	NM_177086	2.3	2.26E−04
Top down-regulated genes				
Thrombospondin 1	*Thbs1*	NM_011580	−9.5	3.24E−06
Left-right determination factor 2	*Lefty2*	NM_177099	−5.4	2.03E−06
Deubiquitinating enzyme 1	*Dub1*	NM_007887	−5.0	2.00E−04
Phospholipase A2, group IB, pancreas	*Pla2g1b*	NM_011107	−4.7	1.45E−03
Transgelin	*Tagln*	NM_011526	−4.6	2.71E−07
Polycystic kidney and hepatic disease 1	*Pkhd1*	NM_153179	−4.6	3.65E−07
Paired-like homeodomain transcription factor 2	*Pitx2*	NM_011098	−4.5	5.18E−05
Left right determination factor 1	*Lefty1*	NM_010094	−4.5	2.82E−06
Actin, alpha 2, smooth muscle, aorta	*Acta2*	NM_007392	−4.4	3.43E−07
Gene model 177, (NCBI)	*Gm177*	XM_134580	−4.3	4.38E−04

LY294002 did not alter expression of chromobox proteins that compose the Polycomb Repressive Complex 1 responsible for binding to methylated histones within promoter regions of affected target genes.

At the same time, treatment with LY294002 resulted in significant inhibition of expression of *Nuclear receptor-binding SET-domain protein 1* (*Nsd1*) and *SET domain containing lysine methyltransferase 7* (*Setd7*), which methylates histone H3 on Lys-36 and Lys-4, respectively, specific tags for transcriptional activation (Supplementary Table II) but did not alter expression of other SET-domain enzyme genes.

The treatment with LY294002 affected not only transcription of lysine methyltransferases but also expression of both histone and non-histone arginine methyltransferases (Supplemental Table II). Although LY294002 did not change expression of *Coactivator-associated arginine methyltransferase 1* (*Carm1*), it modulated transcription of *Protein arginine N-methyltransferase 1 and 5* (*Prmt1* and *Prmt5*) involved in histone methylation and significantly decreased expression of *Jumonji domain containing 6* (*Jmjd6*), which encodes histone demethylase for H3 at Arg-3 and H4 at Arg-4.

LY294002 did not change expression of transcription co-activator genes encoding histone acetyltransferases p300 and CBP but significantly up-regulated transcription of *lysine acetyltransferase 5* (*Htatip*), *lysine acetyltransferase 2A* (*Gcn5*), and *2B* (*pCaf*), and inhibited expression of *Histone aminotransferase 1* (*Hat1*) (Supplemental Table II). Hat1 is the sole representative of the type B histone acetyltransferases and is distinguished from other histone acetyltransferases by its substrate specificity and subcellular localization: this enzyme can be found in the cytoplasm and, most importantly, has the ability to acetylate free, but not nucleosomal histones.

LY294002 did not change transcription of the core class I histone deacetylases (HDACs) or transcription of the components of other repressive complexes such as Sin3, NuRD, CoREST, and N-CoR/SMRT (Supplemental Table II). The only exception is RbAp48, which is not only a component of co-repressor complexes but is also known as retinoblastoma binding protein and, therefore, its transcriptional repression by LY294002 could be a part of PI3K-dependent cell cycle regulation discussed above. Among other HDACs, the LY294002 treatment showed a statistically significant up-regulation for *Hdac5* and *Hdac11* (Supplemental Table II). LY294002 increased also expression of non-histone NAD-dependent deacetylase *sirtuin 1* (*SIRT1*) gene (Supplemental Table II).

Finally, because methylation of DNA and histones are often coordinated, we analyzed expression of DNA-methylating enzymes in the LY294002-treated mESC. We have detected a slight but statistically significant increase in expression of *DNA methyltransferases 1* (*Dnmt1*) and *3A* (*Dnmt3a*), which are responsible for the establishment and maintenance of the DNA methylation pattern in development (Supplemental Table II). We noticed that up-regulation of *Dnmt3a* was accompanied by significant down-regulation of *DNA methyltransferase 3B* (*Dnmt3b*), also required for de novo methylation. LY294002 did not affect expression of *DNA methyltransferase 3-like* (*Dnmt3l*), a component of the NuA4 histone acetyltransferase complex.

GENOME-WIDE CHANGES INDUCED BY ABROGATION OF TFII-I PROTEINS

Next, effects of abrogation of TFII-I proteins on cellular gene expression were determined by Affymetrix expression analysis in comparison with control non-targeting (negative) siRNA. Knockdown of BEN or TFII-I did not cause significant changes in either the number or the ratio of activated to repressed genes (Fig. 2B). However, comparison of list of affected genes ($P < 0.01$) showed that both knockdowns altered profiles of gene expression induced by LY294002 treatment (Fig. 2C). A similar picture was obtained for $P < 0.001$ (data not shown). We noticed that TFII-I knockdown caused more changes in the composition of regulated genes that BEN knockdown, which retained larger number of common genes (77%

vs. 26%) compared to the list of genes induced by LY294002 in the presence of negative control siRNA (Fig. 2C).

Our results revealed differential expression of 208 genes as a result of BEN knockdown and 76 genes as a result of TFII-I knockdown ($corp < 0.25$) in comparison with the negative control siRNA. The lists of up- and down-regulated genes with the highest fold changes are shown in Table II.

In some cases TFII-I proteins work either synergistically or as counterparts regulating common gene targets. We overlapped the list of TFII-I and BEN targets to find genes that are regulated by both transcription factors (Fig. 2C). Among differentially expressed genes 25 were common in both TFII-I and BEN list (Table III), while 183 genes were BEN dependent and 51 genes were regulated by TFII-I only. Twenty-four of these 25 genes displayed the same mode of regulation (up-regulation or down-regulation).

TABLE II. Differentially Expressed Genes With Highest Fold Difference After BEN Knockdown

Gene symbol	Accession #	Fold change	*P*-value
Up-regulated			
Zfp352	NM_153102	3.19	3.19E−05
Gm7969	XM_001473218	2.93	8.02E−05
Ddr2	NM_022563	2.41	3.03E−04
B930075F07	AK147435	1.85	1.03E−04
Gm9720	XM_001477594	1.75	2.69E−04
Ccar1	NM_026201	1.73	7.61E−04
Snapc3	NM_029949	1.73	5.74E−04
C130092O11Rik	XM_908676	1.70	3.15E−04
Lamp2	NM_010685	1.69	5.73E−05
Ninj2	NM_016718	1.66	8.64E−04
Tmem123	NM_133739	1.64	7.64E−05
4933408N05Rik	AK016745	1.62	2.05E−05
A430108E01Rik	NM_001033637	1.61	1.37E−04
Ino80	NM_026574	1.56	1.24E−05
Lamp2	NM_010685	1.55	2.54E−06
Cast	NM_009817	1.54	6.86E−04
Zfp704	NM_133218	1.54	9.55E−04
Sash1	NM_175155	1.52	1.10E−04
Ncoa3	NM_008679	1.52	2.26E−04
Sh3d1B	NM_011365	1.50	4.16E−04
Down-regulated			
Thbs1	NM_011580	−3.62	1.87E−04
Acat1	NM_144784	−1.85	3.14E−04
Tmco7	NM_173037	−1.80	4.22E−04
Slc9a6	NM_172780	−1.79	9.09E−06
Cdc42	NM_009861	−1.66	1.42E−04
Reck	NM_016678	−1.64	7.26E−05
Zfp871	NM_172458	−1.63	2.05E−04
Apoa1	NM_009692	−1.63	1.12E−03
Kbtbd2	NM_145958	−1.62	1.54E−07
1700034H14Rik	NM_025969	−1.56	3.47E−05
Ube2d2	NM_019912	−1.54	7.35E−06
Rpa3	NM_026632	−1.54	2.49E−07
Trim71	NM_001042503	−1.53	1.03E−04
Rnf6	NM_028774	−1.52	3.80E−05
Scrn3	NM_029022	−1.52	1.23E−03

TABLE III. Differentially Expressed Genes With Highest Fold Difference After TFII-I Knockdown

Gene symbol	Accession #	Fold change	*P*-value
Up-regulated			
Gfra2	NM_008115	2.50	6.21E−05
Lamp2	NM_010685	1.64	8.48E−05
Tmem123	NM_133739	1.60	1.06E−04
Lrrc34	XM_487721	1.52	9.41E−05
Down-regulated			
Pigk	NM_025662	−2.44	1.11E−05
Dcp2	NM_027490	−1.75	2.84E−07
Tdp1	NM_028354	−1.68	3.13E−05
Nudt9	NM_028794	−1.63	1.02E−04
Sel1h	NM_011344	−1.59	2.19E−05
Akirin1	NM_023423	−1.55	1.36E−04
Timm8a	NM_013898	−1.55	2.01E−06
Cass4	XM_283813	−1.54	4.84E−06
Nhp2l1	NM_011482	−1.51	4.13E−06

GENOME-WIDE PROMOTER ChIP-Chip ANALYSIS

Zfp352 displays the highest up-regulation upon BEN knockdown. It is one of a few genes, which is temporarily expressed during mouse preimplantation development between the two- and eight-cell embryonic stages [Choo et al., 2001]. The same is true for some other genes significantly up-regulated upon BEN knockdown: analysis of data from GEO record GDS814 reveals that *Gm10454/Chic1* and BG066901 are highly expressed in the mouse morula at the two-cell stage but silent in blastocysts (Fig. 3). *C130092O11Rik/Fam190a* displays a strong expression in oocytes and early morula development until the eight-cell stage. This suggests specific repressive function of BEN for such genes. In contrast, expression of *Zinc finger protein 871* (*Zfp871*) is increased during early embryonic development with the highest expression in blastocysts (Fig. 3).

Genome-wide promoter ChIP-chip results indicated that the majority of genes differently expressed after abrogation of *Gtf2i* and *Gtf2ird1* could be direct targets of TFII-I or BEN transcriptional regulation. Namely, chromatin immunoprecipitation with anti-BEN polyclonal antibodies following analysis of mouse 385K Promoter Arrays revealed that 66.5% of genes that changed their expression upon *Gtf2ird1* knockdown had more than a 1.5-fold enrichment of BEN binding within 2 kb of their promoter regions. Representative examples of such genes are shown in Figure 4. Similarly, 94% of genes whose expression was changed after *Gtf2i* knockdown had more than a 1.5-fold enrichment of TFII-I binding across their promoters. Furthermore, many high-confidence binding peaks coincided with the canonical TFII-I binding core consensus RGATTR [Vullhorst and Buonanno, 2005] in promoters of both up- and down-regulated genes suggesting them to be direct transcriptional targets of TFII-I factors.

The promoter ChIP-chip analysis confirmed BEN recruitment to the chromatin region near the transcription start site of *Zfp871* (Fig. 4A). This binding peak coincides with the sequence AGATTG corresponding to the consensus RGATTR motif. *Lamp2*, *Tmeme123*, and *Plgk* are another examples of TFII-I and BEN occupancy within their regulatory regions (Fig. 4).

DISCUSSION

The effect of inhibition of PI3K/Akt signaling on gene expression in mESC using the Affymetrix platform has been previously published [Storm et al., 2009]. Although our primary interest was to study the contribution of TFII-I proteins in the mESC differentiation, we found 206 genes, which comprise 41% of all previously reported genes,

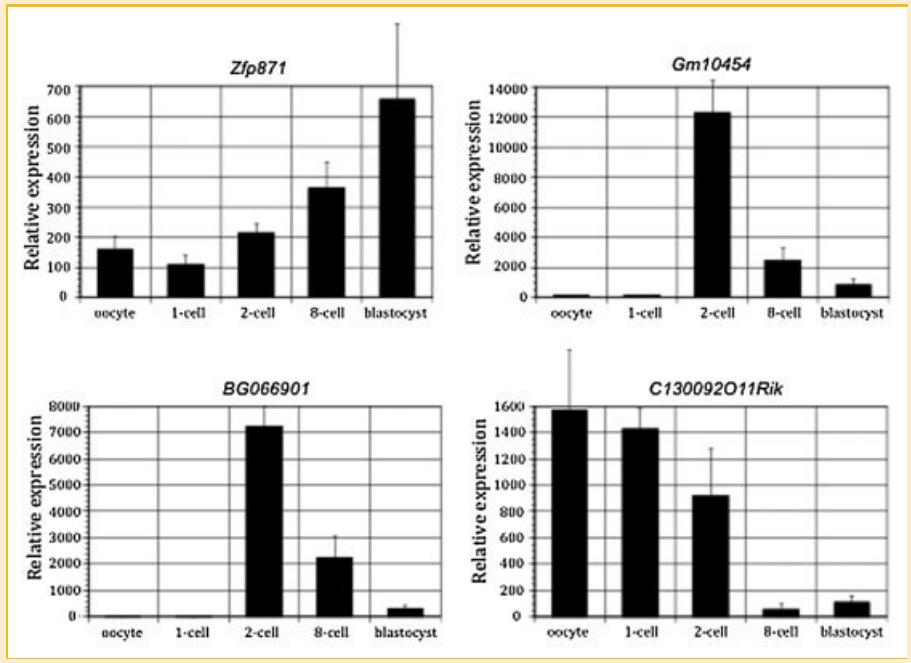

Fig. 3. Expression pattern of genes in preimplantation mouse embryos down-regulated (*Zfp871*) or up-regulated (*Gm10454*/*Chic1*, BG066901, and *C130092O11Rik*/*Fam190a*) by BEN knockdown in mESCs in the presence of 5 μM LY294002. Data from GEO record GDS814.

affected by inhibition of PI3K/Akt [Storm et al., 2009]. There are several reasons that may have contributed to differences between the affected genes in the two studies. First, our experimental condition differed from theirs in terms of cell density which could significantly influence subsequent differentiation outcomes; second, we used different labeling and data analysis approaches; third, possible off-target effects from negative control siRNA used in our study for comparison with untreated mESC could account for the differences. Before discussion of the expression changes in mESC induced by abrogation of TFII-I proteins, we will describe the inhibiting effects of PI3K/Akt signaling deduced from our analysis which complement previously published studies.

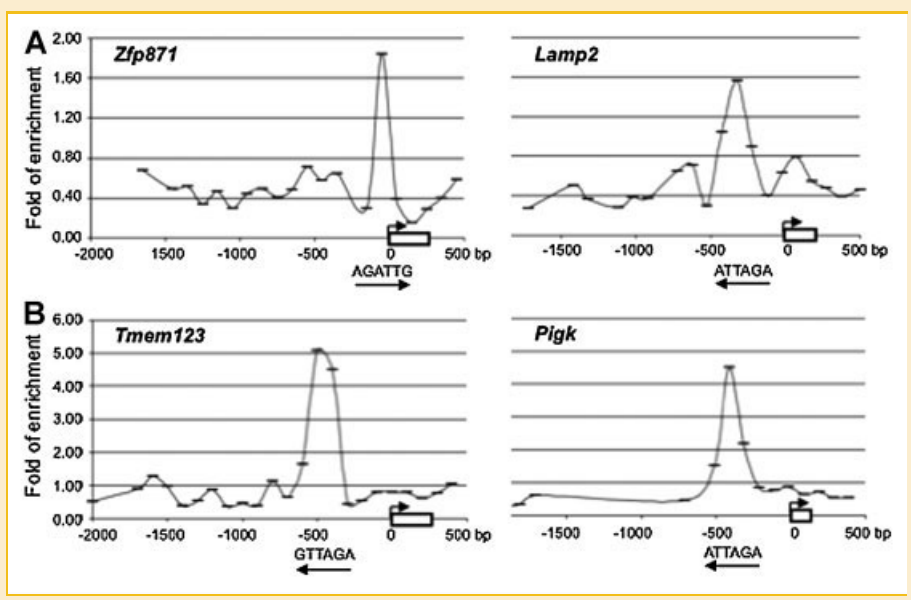

Fig. 4. Binding profiles of BEN (A) and TFII-I (B) in promoter regions of representative up-regulated (*Lamp2* and *Tmem123*) and down-regulated (*Pigk* and *Zfp871*) genes. Data were obtained in the genome-wide promoter ChIP-chip experiments. Positions of symbols correspond to location of tiling oligonucleotide probes and relative intensity of their hybridization with immunoprecipitated DNA fragments.

EFFECTS OF LY294002 INHIBITION OF THE PI3K PATHWAY ON CELL CYCLE

Characteristic features of mESC are the short duration of their cell cycle, mainly as a result of the shortened G_1 phase, and the capability to proliferate in the absence of external mitogenic factors. In somatic cells, the $G_1 \rightarrow S$ transition is regulated by both ERK and PI3K pathways, whereas in mESC inhibition of the ERK pathway does not affect cycle progression but inhibition of the PI3K pathway with 40 μM LY294002 leads to a twofold increase of the G_1/S ratio [Lianguzova et al., 2007]. Delayed enter into S phase in LY249002-treated mESC occurs with down-regulation of the transcriptional activity of cyclin-kinase complexes and E2F factors: cyclin D1, cyclin E, E2F factors and Cdk2 are decreased, whereas the amount of Cdk4 protein and transcription of *p27Kip1* did not change significantly [Lianguzova et al., 2007]. Our expression profiling gives almost the same results but provides a more complete picture of transcriptional changes of genes involved in the cell cycle regulation.

Reduced luciferase activity under the E2F-responsive promoter was detected after treatment of mESC with 40 μM LY29002 [Lianguzova et al., 2007]. However, our data show that regulation of endogenous E2F genes is more complicated in mESC. After treatment of cells with 5 μM LY29002, microarray profiling revealed (with the exception of *E2f3*) either the absence of transcriptional changes (*E2f2*, *E2f4*, *E2f5*, and *E2f7*) or a weak increase in expression (*E2f1* and *E2f6*) of E2F genes (Supplementary Table I). Together with a significant decrease of retinoblastoma (*Rb*) expression (Supplementary Table I), these data explain why the low concentration of LY29002 (5 μM) does not inhibit growth and proliferation of mESC despite transcriptional changes of the Cyclin/Cdk/Cdkn components described above. Thus, our analysis suggests that (i) in mESC the PI3K pathway regulates assembly and activity of cyclin D-Cdk4/6 but not of cyclin E-Cdk2 complexes, and (ii) PI3K controls expression of both activating (cyclins D1 and D2) and inhibiting (Cdkn1a and Cdkn1c) subunits of the cyclin-dependent protein kinase complexes thus setting the limits on regulation of their activity.

The role of the PI3K/Akt pathway in cell cycle regulation of ESC as well as the evidence that Gsk3 and Nanog are key players in this pathway was demonstrated previously in several publications [Jirmanova et al., 2002; Sato et al., 2004; Storm et al., 2007; Ying et al., 2008; Bone et al., 2009; Lui et al., 2009]. Therefore here we focus our attention on discussion of differentiation processes and epigenetic modifications that takes place as a result of PI3K inhibition and the contribution of TFII-I proteins to these processes.

EFFECTS OF LY29002 TREATMENT ON CHROMATIN REMODELING ENZYME GENES

Although we failed to detect a decrease of pluripotency markers or increase in expression of early markers of differentiation in short-treatment experiments, epigenetic reprogramming of differentiation could have been started before expression alterations. In addition, because chromatin is dynamically restructured during each mitotic cycle, comparative examination of epigenetic changes in LY294002-treated ES cells provides specific information about functioning of the cell cycle. Therefore, we have analyzed expression of a complete spectrum of histone methyltransferases, demethylases, acetyltransferases, deacetylases, and DNA methyltransferases as well as proteins interacting with these enzymes in the content of multicomponent complexes. Results indicate that LY294002 treatment has significant and specific effects on expression of several key chromatin-modifying enzymes (Supplementary Table II).

In the LY294002-treated mESC, we found an increased expression of *Suv39h1*, which is involved in the establishment of constitutive heterochromatin at pericentric and telomeric regions. Histone H3 tails methylated at Lys-9 by Suv39h1 recruit chromobox proteins, expression of which was also affected by LY29002 treatment. We have detected modest but statistically significant up-regulation of *Cbx5* (*heterochromatin protein 1 homolog alpha*), which is responsible for the formation of functional kinetochore during cell division, and of *Cbx3* (*heterochromatin protein 1 homolog gamma*), mainly responsible for association of heterochromatin with the inner nuclear membrane. Expression of *Cbx1* (*heterochromatin protein 1 homolog beta*), which is associated with centromeres, was decreased in LY294002-treated mESC.

Beyond potentially affecting heterochromatin in dividing cells, LY294002 treatment demonstrated significant and consistent changes in expression of some key enzymes involved in epigenetic transcriptional regulation of target genes within euchromatin (Supplemental Table II). We observed both up-regulation of enzymes generating specific tags for transcriptional repression (*Ehmt2* and *Ezh2*) and down-regulation of enzymes generating specific tags for transcriptional activation (*Nsd1* and *Set7*).

The LY294002 treatment of mESC slightly enhanced expression of *F-box* and *leucine-rich repeat protein 10* (*Fbxl10*), which preferentially demethylates at H3 Lys-36 (Supplementary Table I). This suggests that decreased methylation of Lys-36 was accompanied by erasing these activation marks at H3K36. In contract, transcription activity of *Amine oxidase* (*flavin containing*) *domain 2* (*Aof2*), which specifically demethylates Lys-4 of histone H3, was decreased in the inhibitor-treated mESC.

Effects of LY294002 treatment on histone tags for transcriptional repression are more complicated. Inhibition of PI3K/Akt pathway can increase generation of methylated H3K9 and H3K27 as a result of activated transcription of *Ehmt2* and *Ezh2* methyltransferases, consistent with the observation that AKT phosphorylates EZH2 at Ser-21 and suppresses its methyltransferase activity by impeding EZH2 binding to histone H3 resulting in a decrease of Lys-27 trimethylation and derepression of silenced genes [Cha et al., 2005]. However, the level of methylated H2K9 tags can also be affected by increased expression of histone demethylase *Jumonji domain containing 1A* (*Jmjd1a*) and by decreased expression of *Jumonji domain containing 2B* (*Jmjd2b*) (Supplemental Table II). In addition, LY294002 treatment significantly inhibited expression of *PR domain containing 2 with ZNF domain* (*Prdm2/Riz1*), which encodes histone methyltransferase, which specifically methylates Lys-9 of histone H3 (Supplemental Table II). However, this protein can also play a role as a tumor suppressor in pathogenesis of retinoblastoma, so alteration of its transcription activity could be linked to cell cycle regulation rather than to epigenetic reprogramming of target gene expression.

LY294002 treatment also appeared to affect cellular memory of recent transcriptional activity. Although expression of the gene for the DOT1-like histone H3 (DOT1l) methyltransferase, which modifies Lys-79 of histone H3, did not change, we have detected decreased expression of *Setdb1* which encodes the catalytic subunit of one of SET1 complexes, as well as transcriptional activation of *SET* and *MYND domain containing 1* (*Smyd1*) and *3* (*Smyd3*), that induce di- and trimethylation of Lys-4 of histone H3 and are also associated with elongating RNA polymerase complexes (Supplemental Table II).

Acetylation of histones gives more specific tags for epigenetic transcription activation and, indeed, we have found histone acetyltransferases among LY294002-affected genes. Namely, LY294002 up-regulates transcription of *Gcn5*, which encodes a component of the TFTC-HAT and STAGA transcription coactivator–HAT complexes and has significant histone acetyltransferase activity with core histones, but not with nucleosome core particles, and of pCaf, which has histone acetyltransferase activity both with core histones (H3 and H4) and with nucleosome core particles. pCaf inhibits cell-cycle progression and counteracts the mitogenic activity of the adenoviral oncoprotein E1A. In addition, LY294002 treatment increased expression of *Htatip*, which is a catalytic subunit of the NuA4 histone acetyltransferase complex. This complex may be required for the activation of transcriptional programs associated with oncogene and proto-oncogene mediated growth induction, tumor suppressor mediated growth arrest and replicative senescence, apoptosis, and DNA repair.

Among all of the genes for histone-modifying enzymes, LY294002 exerts the smallest effects on HDACs: only *Hdac5* and *Hdac11* showed statistically significant up-regulation. Both HDAC5, which functions as an adaptor to nucleate multiple types of transcriptional regulators, and HDAC11, which is structurally different from other enzymes and represents the sole class IV HDAC, show relatively restricted expression patterns and are highly enriched in muscles, heart, and brain [Zhang et al., 2002; Chang et al., 2004; Liu et al., 2008]. Stimulation of their transcription activity by LY294002 suggests that *Hdac5* and *Hdac11* may be negatively regulated by PI3K in these tissues.

Based on the collected evidence we conclude that the PI3K/Akt pathway may have specific epigenetic effects on both histone methylation and acetylation. However, epigenetic activation and repression of target genes in the LY294002-treated mESC is achieved, in general, by different mechanisms: transcriptional repression is mainly orchestrated through the histone methylation status, while transcription activation is a response to specific histone acetylation events.

GENE EXPRESSION CHANGES INDUCED BY ABROGATION OF TFII-I PROTEINS

By abrogation of *Gtf2i* and *Gtf2ird1*, we investigated how TFII-I and BEN might be involved in process of mESC differentiation. Because activation of Akt signaling is sufficient to maintain pluripotency in mESC in the absence of LIF and significantly down-regulates expression of *Gtf2i* and *Gtf2ird1* we speculate that up-regulation TFII-I proteins is necessary to activate specific sets of genes during early mESC differentiation. We predicted that inhibition of the PI3K/Akt pathway by LY294002 increases expression of *Gtf2i* and *Gtf2ird1* and activates expression of the TFII-I target genes in mESC. Therefore we expected that the siRNA-induced knockdown of TFII-I proteins along with LY294002 treatment would identify genes, activation of which in differentiating mESC is dependent on TFII-I and BEN.

Although after 24 h of gene-specific siRNA treatments we detected neither a significant decrease of pluripotency markers nor an increase in expression of known markers of differentiation, some genes showed an immediate and significant up-regulation (Table II). However, effects of TFII-I knockdown on gene expression in mESC are less prominent than those of BEN (Table II and Fig. 2B). This could be explained by the fact that TFII-I is a phosphoprotein in contrast to BEN and needs additional activation by a specific phosphorylation to exert its regulatory action.

Zfp352 demonstrates the highest activation upon BEN knockdown. The function of this gene remains largely unknown, but it is one of a few genes, which is temporarily expressed during mouse preimplantation development between the two- and eight-cell embryonic stages [Choo et al., 2001]. The same is true for some other genes significantly up-regulated upon BEN knockdown: analysis of data from GEO record GDS814 reveals that *Gm10454/Chic1*, BG066901, and *C130092O11Rik/Fam190a* are temporary expressed in the mouse morula but silent in blastocysts (Fig. 3). This suggests specific repressive function of BEN for such genes. In contrast, *Zinc finger protein 871* (*Zfp871*) is normally expressed in blastocysts (Fig. 3) and is down-regulated by BEN abrogation in mESC. Promoter ChIP-chip analysis confirmed BEN recruitment to the region near the transcription start site of *Zfp871*, and this binding peak coincides with the sequence AGATTG corresponding to the consensus RGATTR motif (Fig. 4A). Moreover, ChIP-chip data indicated that a large set of genes differently expressed after abrogation of *Gtf2i* and *Gtf2ird1* could be direct targets of TFII-I proteins (Fig. 4).

Regarding epigenetic changes in mESC, BEN knockout resulted in lower expression of *Ehmt1* encoding Euchromatic histone methyltransferase 1, which represses transcription by methylation of H3K9 (Supplemental Table II). Moreover, BEN knockdown reduced expression of *Ezh2*, another key repressive methyltransferase gene, even in spite of up-regulation of *Ezh2* expression by LY294002 treatment (Supplemental Table II). In general, knockdowns of TFII-I proteins not only impeded PI3K/Akt-dependent expression for some genes but also, in some cases, reversed these changes as has been shown for the *Ezh2* gene. However, further studies are clearly required to better define the spectrum of immediate TFII-I gene targets in the early mESC differentiation.

CONCLUSIONS

We have extended previously published data on role of the PI3K/Akt pathway in cell proliferation and self-renewal to show that inhibition of PI3K in mESC resulted in significant changes in expression of a specific subset of chromatin-modifying enzymes. Most of the predicted epigenetic alterations resulting from regulation of these enzymes are linked to cell cycle functioning

in the LY294002-treated mESC, although some of them (for example, such as transcriptional activation of *Moz* and *Morf*) could reflect the beginning of mESC differentiation induced by LY294002 treatment. Our gene profiling analyses also supports the idea that up-regulation of TFII-I proteins interferes with the role of the PI3K/Akt pathway during mESC self-renewal.

ACKNOWLEDGMENTS

This work was supported by the NIH grants R01DE017205 and K02 DE18412 and Connecticut Stem Cell Grant 09-SCB-UCHC to D.B. We thank Dr. William Upholt for helpful discussions and comments on the manuscript.

REFERENCES

Bayarsaihan D, Bitchevaia N, Enkhmandakh B, Tussie-Luna MI, Leckman JF, Roy A, Ruddle F. 2003. Expression of BEN, a member of TFII-I family of transcription factors, during mouse pre- and postimplantation development. Gene Expr Patterns 3:579–589.

Bone HK, Damiano T, Bartlett S, Perry A, Letchford J, Ripoll YS, Nelson AS, Welham MJ. 2009. Involvement of GSK-3 in regulation of murine embryonic stem cell self-renewal revealed by a series of bisindolylmaleimides. Chem Biol 16:15–27.

Cha TL, Zhou BP, Xia W, Wu Y, Yang CC, Chen CT, Ping B, Otte AP, Hung MC. 2005. Akt-mediated phosphorylation of EZH2 suppresses methylation of lysine 27 in histone H3. Science 310:306–310.

Chang S, McKinsey TA, Zhang CL, Richardson JA, Hill JA, Olson EN. 2004. Histone deacetylases 5 and 9 govern responsiveness of the heart to a subset of stress signals and play redundant roles in heart development. Mol Cell Biol 24:8467–8476.

Chimge NO, Makeyev AV, Ruddle FH, Bayarsaihan D. 2008. Identification of the TFII-I family target genes in the vertebrate genome. Proc Natl Acad Sci USA 105:9006–9010.

Choo KB, Chen HH, Cheng WT Chang HS, Wang M. 2001. *In silico* mining of EST databases for novel pre-implantation embryo-specific zinc finger protein genes. Mol Reprod Dev 59:249–255.

Djordjevic S, Driscoll PC. 2002. Structural insight into substrate specificity and regulatory mechanisms of phosphoinositide 3-kinases. Trends Biochem Sci 27:426–432.

Enkhmandakh B, Bitchevaia N, Ruddle F, Bayarsaihan D. 2004. The early embryonic expression of TFII-I during mouse preimplantation development. Gene Expr Patterns 4:25–28.

Enkhmandakh B, Makeyev AV, Erdenechimeg L, Ruddle FH, Chimge NO, Tussie-Luna MI, Roy AL, Bayarsaihan D. 2009. Essential functions of the Williams-Beuren syndrome-associated TFII-I genes in embryonic development. Proc Natl Acad Sci USA 106:181–186.

Ferrero GB, Howald C, Micale L Biamino E, Augello B, Fusco C, Turturo MG, Forzano S, Reymond A, Merla G. 2010. An atypical 7q11.23 deletion in a normal IQ Williams-Beuren syndrome patient. Eur J Hum Genet 18:33–38.

Jirmanova L, Afanassieff M, Gobert-Gosse S, Markossian S, Savatier P. 2002. Differential contributions of ERK and PI3-kinase to the regulation of cyclin D1 expression and to the control of the G1/S transition in mouse embryonic stem cells. Oncogene 21:5515–5528.

Lianguzova MS, Chuykin IA, Nordheim A, Pospelov VA. 2007. Phosphoinositide 3-kinase inhibitor LY294002 but not serum withdrawal suppresses proliferation of murine embryonic stem cells. Cell Biol Int 31:330–337.

Lui N, Lu M, Feng XM, Ma FX, Fang ZH, Tian XM, Ren Q, Zhang L, Liu B, Huang PP, Liu L, Han ZC. 2009. Exogenous Nanog alleviates but is insufficient to reverse embryonic stem cells differentiation induced by PI3K signaling inhibition. J Cell Biochem 106:1041–1047.

Liu H, Hu Q, Kaufman A D'Ercole AJ, Ye P. 2008. Developmental expression of histone deacetylase 11 in the murine brain. J Neurosci Res 86:537–543.

Paling NR, Wheadon H, Bone HK, Welham MJ. 2004. Regulation of embryonic stem cell self-renewal by phosphoinositide 3-kinase-dependent signaling. J Biol Chem 279:48063–48070.

Tassabehji M, Hammond P, Karmiloff-Smith A, Thompson P, Thorgeirsson SS, Durkin ME, Popescu NC, Hutton T, Metcalfe K, Rucka A, Stewart H, Read AP, Maconochie M, Donnai D. 2005. GTF2IRD1 in craniofacial development of humans and mice. Science 310:1184–1187.

Sato N, Meijer L, Skaltsounis L, Greengard P, Brivanlou AH. 2004. Maintenance of pluripotency in human and mouse embryonic stem cells through activation of Wnt signaling by a pharmacological GSK-3-specific inhibitor. Nat Med 10:55–63.

Stewart MH, Bendall SC, Bhatia M. 2008. Deconstructing human embryonic stem cell cultures: Niche regulation of self-renewal and pluripotency. J Mol Med 86:875–886.

Shen X, Liu Y, Hsu TJ, Fujiwara Y, Kim J, Mao X, Yuan GC, Orkin SH. 2008. EZH1 mediates methylation on histone H3 lysine 27 and complements EZH2 in maintaining stem cell identity and executing pluripotency. Mol Cell 32:491–502.

Storm MP, Bone HK, Beck CG, Bourillot PY, Schreiber V, Damiano T, Nelson A, Savatier P, Welham MJ. 2007. Regulation of Nanog expression by phosphoinositide 3-kinase-dependent signaling in murine embryonic stem cells. J Biol Chem 282:6265–6273.

Storm MP, Kumpfmueller B, Thompson B, Kolde R, Vilo J, Hummel O, Schulz H, Welham MJ. 2009. Characterization of the phosphoinositide 3-kinase-dependent transcriptome in murine embryonic stem cells: Identification of novel regulators of pluripotency. Stem Cells 27:764–775.

Vullhorst D, Buonanno A. 2005. Multiple GTF2I-like repeats of general transcription factor 3 exhibit DNA-binding properties: Evidence for a common origin as a sequence-specific DNA interaction module. J Biol Chem 280:31722–31731.

Watanabe S, Umehara H, Murayama K, Okabe M, Kimura T, Nakano T. 2006. Activation of Akt signaling is sufficient to maintain pluripotency in mouse and primate embryonic stem cells. Oncogene 25:2697–2707.

Yoshikawa T, Piao Y, Zhong J, Matoba R, Carter MG, Wang Y, Goldberg I, Ko MS. 2006. High-throughput screen for genes predominantly expressed in the ICM of mouse blastocysts by whole mount in situ hybridization. Gene Expr Patterns 6:213–224.

Ying QL, Wray J, Nichols J, Batlle-Morera L, Doble B, Woodgett J, Cohen P, Smith A. 2008. The ground state of embryonic stem cell self-renewal. Nature 453:519–523.

Zhang CL, McKinsey TA, Chang S, Antos CL, Hill JA, Olson EN. 2002. Class II histone deacetylases act as signal-responsive repressors of cardiac hypertrophy. Cell 110:479–488.